

RESEARCH

Open Access



Risk stratification of lung adenocarcinoma using a nomogram combined with ferroptosis-related LncRNAs and subgroup analysis with immune and N6-methyladenosine modification

Chen Gao^{1,2†}, Ning Kong^{1,2†}, Fan Zhang^{1,2}, Tianyu Tang^{3,4}, Jiaying Li^{1,2}, Honglei Ding^{1,2}, Zhichao Sun^{1,2}, Linyu Wu^{1,2*} and Maosheng Xu^{1,2*}

Abstract

Background: Determining the prognosis of lung adenocarcinoma (LUAD) is challenging. The present study aimed to identify prognostic ferroptosis-related long noncoding RNAs (FRLs) and construct a prognostic model. Moreover, differential analysis of immune and N6-methyladenosine (m6A)-related genes was systematically conducted.

Methods: A total of 504 patients selected from a dataset from The Cancer Genome Atlas were included. The patients with LUAD were randomly divided into a training group and a test group at a ratio of 1:1. Pearson correlation analysis and univariate Cox regression analysis were used to identify the prognostic FRLs. Then, a prognostic model was constructed from the optimized subset of prognostic FRLs based on the least absolute shrinkage and selection operator (LASSO) algorithm. Subsequently, the receiver operating characteristic (ROC) curve and survival analysis were used to evaluate the performance of the model. The risk score based on the prognostic model was analyzed using Cox regression analysis. Moreover, gene set enrichment analysis and differential analysis of immune- and m6A-related genes were conducted.

Results: After univariate Cox regression analysis and LASSO algorithm analysis, a total of 19 prognostic FRLs were selected to construct the final model to obtain the risk score. The area under the ROC curve of the prognostic model for 1-year, 3-year, and 5-year overall survival (OS) was 0.763, 0.745, and 0.778 in the training set and 0.716, 0.724, and 0.736 in the validation set, respectively. Moreover, the OS of the high-risk group was significantly worse than that of the low-risk group in the training group ($P < 0.001$) and in the test group ($P < 0.001$). After univariate and multivariate Cox regression analysis, the risk score [hazard ratio (HR) = 1.734; $P < 0.001$] and stage (HR = 1.557; $P < 0.001$) were both considered significant prognostic factors for LUAD. A nomogram was constructed based on clinical features and risk

*Correspondence: wulinyu@zcmu.edu.cn; xums166@zcmu.edu.cn

†Chen Gao and Ning Kong have contribute equally to this work

¹ Department of Radiology, The First Affiliated Hospital of Zhejiang Chinese Medical University (Zhejiang Provincial Hospital of Traditional Chinese Medicine), 54 Youdian Road, Hangzhou, China

Full list of author information is available at the end of the article



score. The expression of 34 checkpoint genes and 13 m6A-related genes varied significantly between the two risk groups.

Conclusion: This study constructed a prognostic model to effectively predict the OS of patients with LUAD, and these OS-related FRLs might serve as potential therapeutic targets of LUAD.

Keywords: Lung adenocarcinoma, Ferroptosis, N6-methyladenosine, Long noncoding RNA, Prognosis, Biomarker

Background

Lung cancer is a malignancy with high mortality and the second highest incidence worldwide in most countries, with approximately 235,760 new lung cancer cases diagnosed and approximately 131,880 related deaths in 2021 [1]. Generally, the five-year survival of patients with lung cancer ranges from 10 to 20% [2]. Lung adenocarcinoma (LUAD) is the subtype of lung cancer with the highest prevalence [3, 4]. Despite advancements in surgery, radiotherapy, chemotherapy, and other advanced therapeutics, the prognosis remains poor due to the high heterogeneity of LUAD [5, 6]. As such, research into the molecular mechanisms and pathogenesis of LUAD requires further research to develop promising therapies.

Ferroptosis is a specific type of cell death that is typically associated with the accumulation of iron and peroxidation and has been identified as a promising intervention in cancer therapeutics to trigger apoptosis of malignancies that are resistant to traditional methods [7–9]. Ferroptosis-related genes (FRGs) is genes that can promote, prevent or indicate the occurrence of ferroptosis, which annotated as drivers, suppressors or markers [10]. Some studies have even noticed the potential role of FRGs in lung cancer development and suppression, but the specific details remain elusive [11–13]. Long noncoding RNAs (lncRNAs) are a type of noncoding RNA sequence measuring approximately 200 nucleotides in length, and these sequences affect several processes, such as cell growth and apoptosis [14]. The regulation of lncRNAs in ferroptosis has been investigated and found to be related to different malignancies, including lung cancer [15, 16]. However, there are only a few studies on the mechanism of how ferroptosis-related lncRNAs (FRLs) act on the occurrence and progression of LUAD. As such, studies investigating the involvement of FRLs in the development of LUAD may be of great value for identifying potential targets for guided treatment. Separately, N6-methyladenosine (m6A) modification is an important method of RNA posttranscriptional modification in most eukaryotic mRNAs and lncRNAs [17, 18]. Many studies have indicated that m6A modification is related to the oncogenesis and progression of malignant tumors, including LUAD, and could regulate ferroptosis

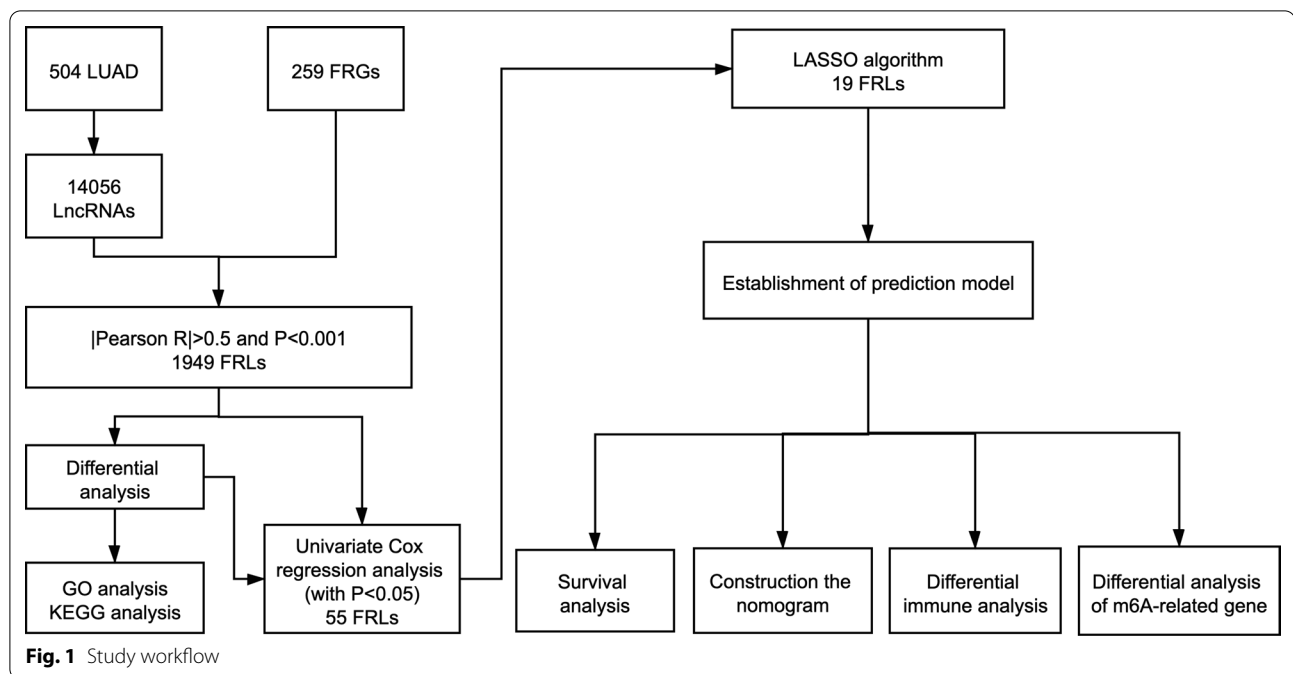
[19–22]. Therefore, it is essential to study these m6A modifications to comprehensively understand the involvement of FRLs in the development of LUAD.

With these important markers in mind, we sought to identify the prognostic value of FRLs using bioinformatics and a statistical analysis of data collected from patients with LUAD from The Cancer Genome Atlas (TCGA) dataset. In addition, a prognostic model will be created using an optimistic subset of FRLs to predict the long-term mortality of LUAD patients and used to construct a nomogram for guiding clinical judgment. Subgroup analysis along with immune and m6A modification will be used in conjunction to further determine the performance of the model and the expression of related genes within the study groups.

Methods

Datasets and FRGs

The study protocol was conducted in accordance with the Declaration of Helsinki. Informed consent was waived owing to the retrospective nature of this study. Transcriptome profiling data [fragments per kilobase of transcript per million mapped reads normalized] and the relevant clinical data were obtained from the Genomic Data Commons Data Portal (<https://portal.gdc.cancer.gov>). The inclusion criteria were as follows: (1) LUAD confirmed by pathology; (2) patients with LUAD who had complete transcriptome profiling data; and (3) patients with LUAD who had complete survival data. The exclusion criteria were as follows: incomplete information of the transcriptome profiling data and clinical data. A total of 504 patients with LUAD were included in this study from the TCGA cohort. A total of 259 FRGs (382 annotations) were included in this study, which were downloaded from the FerrDb database (<http://www.zhounan.org/ferrdb>) and could be divided into drivers, markers and suppressors. The annotation of the lncRNAs in the TCGA dataset was conducted by the annotation file of Genome Reference Consortium Human Build 38 (GRCh38), which was downloaded from the GENCODE website. A total of 14,056 lncRNAs were identified based on recognizing the ensemble IDs of the genes in the TCGA datasets. The flow chart of study is shown in Fig. 1.



Ferroptosis-related lncRNA (FRL) selection and differential expression gene (DEG) analysis

FRLs were initially identified based on the expression of lncRNAs and FRGs by Pearson correlation analysis with $|\text{Pearson } R| > 0.5$ and $P < 0.001$. The different expression levels of FRGs and FRLs were analyzed by Wilcoxon tests between the normal group and the tumor group with \log_2 fold change (FC) > 1 and false discovery rate (FDR) < 0.05 . Gene Ontology (GO) and Kyoto Encyclopedia of Genes and Genomes (KEGG) analyses of these DEGs were performed. Then, the prognostic FRLs were determined by univariate Cox regression analysis from the significantly different expression of FRLs ($P < 0.05$).

Construction of prediction model and validation

The training and test sets of patients with LUAD were randomly classified at a ratio of 1:1. The final prognostic model was constructed using the optimized subset of prognostic FRLs chosen by the least absolute shrinkage and selection operator (LASSO) algorithm. The risk score (RS) was computed by the chosen lncRNA expression weighted by their corresponding coefficients. The prognostic model was then assessed by ROC analysis and a risk plot. Using the median RS, those with LUAD were separated into either high- or low-risk groups. The OS of patients with LUAD in the two-risk group was shown by the Kaplan–Meier (KM) method in the training and test sets and the comparison was conducted. The RS and clinical features of patients with LUAD were analyzed by univariate and multivariate Cox regression analysis. The

differential analysis of each clinical group based on the two-risk group was conducted by the chi-square test. The development of the nomogram was conducted based on RS and clinical features and evaluated by ROC analysis.

Gene set enrichment analysis (GSEA) and differential immune analysis

GSEA was conducted by GSEA software (version 4.1.0) in the two risk groups of LUAD. A p value < 0.05 and the method of signal2noise were selected to denote enrichment significance. Then, the TIMER [23], CIBERSORT [24], CIBERSORT-ABS, QUANTISEQ [25], Microenvironment Cell Populations-counter (MCPOUNTER) [26], XCELL [27] and Estimating the proportion of Immune and Cancer cells (EPIC) [28] tools were used to estimate the abundances of immune cells between the two risk groups. In addition, single sample GSEA was used to quantify the immune cells and the pathways between the two risk groups. The expression levels of immune checkpoint-related genes in the two groups were compared by the Wilcoxon test.

Analysis of m6A-related genes

A total of 23 m6A regulators were identified based on previous literature, which could be divided into writers, erasers and readers. METTL3, METTL14, METTL16, WTAP, VIRMA, RBM15, RBM15B, and ZC3H13 were the regulators as writers. FTO and ALKBH5 were the regulators as erasers. YTHDC1, YTHDC2, YTHDF1, YTHDF2, YTHDF3, HNRNPC, FMR1, LRPPRC,

HNRNPA2B1, IGF2BP1, IGF2BP2, IGF2BP3, and RBMX were the regulators as readers. The expression levels of m6A-related genes in the two-risk group were also compared.

Statistical analysis

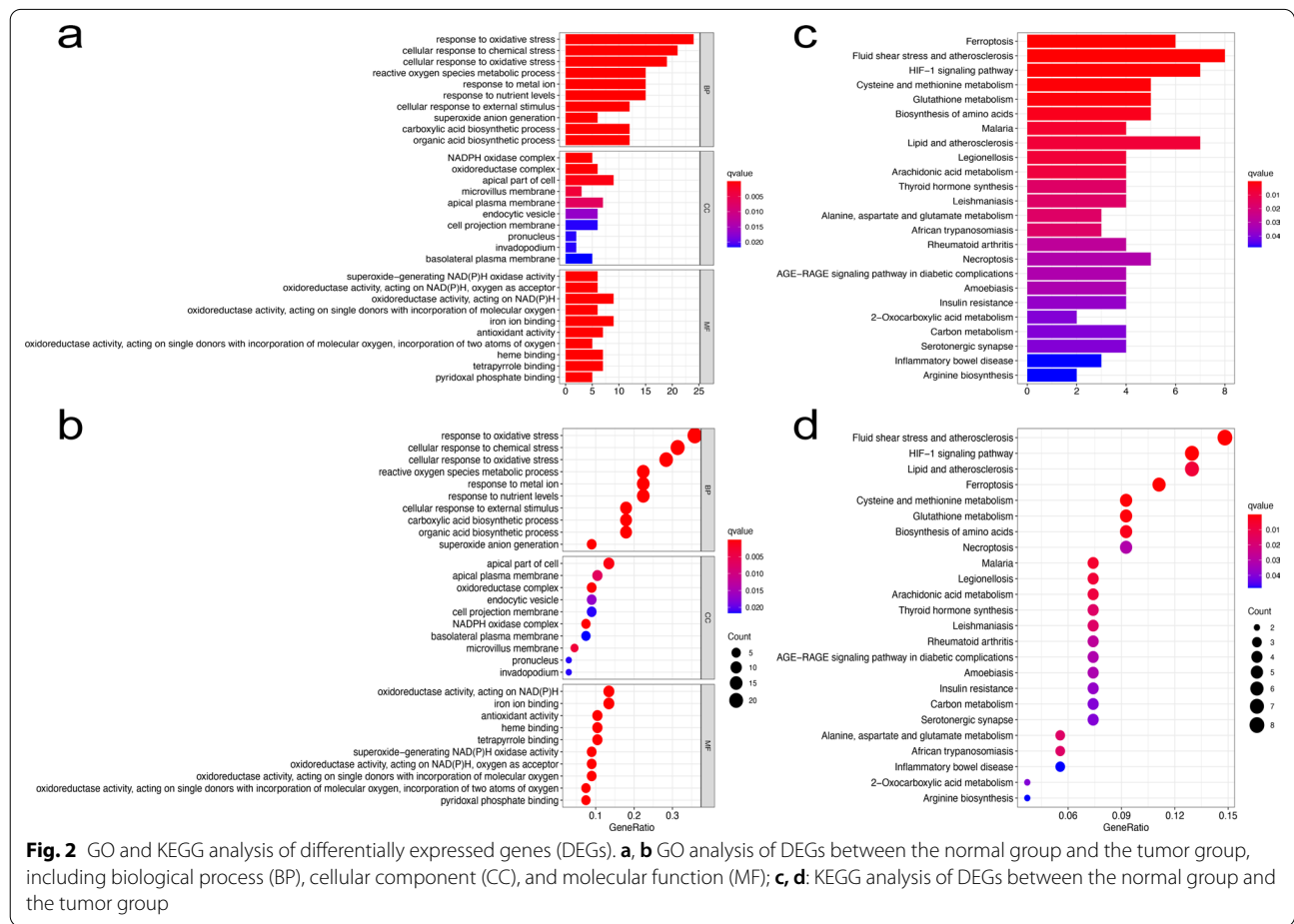
R statistical software (version 4.0.5) was used for all statistical analyses. Student’s t test, Mann–Whitney U test or Kruskal–Wallis H-test was used for continuous variables. A chi-square test or Fisher’s exact test was used for categorical variables. The “limma” package was used to analyze transcriptome profiling data. The “clusterProfiler”, “org.Hs.eg.db”, “enrichplot”, and “ggplot2” packages were used to conduct the GO analysis and KEGG analysis and build bar plots and bubble plots. The “survival”, “survminer”, “caret”, “glmnet” and “timeROC” packages were used to conduct the survival analysis, build the prognostic model and obtain the ROC curve. The “ggalluvial”, “ggplot2”, and “dplyr” packages were used to develop the Sankey diagram. The “pheatmap” package was used to develop heatmaps and risk plots. The “survival” and “regplot” packages were used to develop the nomogram.

The “GSVA”, “GSEABase”, “ggpubr”, and “reshape2” packages were used to develop box plots for the immune function analysis and the differential expression of checkpoint-related genes and m6A-related genes between the two-risk group. A two-sided $P < 0.05$ was considered statistically significant.

Results

Identification of FRLs in LUAD patients

A total of 1949 FRLs were determined by Pearson correlation analysis to be significant (with $|\text{Pearson } R| > 0.5$ and $P < 0.001$). The expression of 70 FRGs and 664 FRLs was significantly different between the normal group and the tumor group. With regard to biological processes, GO was used to enrich the DEGs by biological process (BP), cellular component (CC), and molecular function (MF), as shown in Fig. 2a-b. With regard to BP, these DEGs were mainly enriched in response to oxidative stress and cellular response to chemical stress. With regard to CC, these DEGs were mainly enriched in the NADPH oxidase complex. With regard to MF, these DEGs were mainly enriched in superoxide-generating NADPH oxidase



activity. Furthermore, we used KEGG to conduct pathway analysis on these DEGs and found that the DEGs were mainly enriched in ferroptosis and fluid shear stress and atherosclerosis, as shown in Fig. 2c-d. Then, a total of 55 prognostic FRLs were selected by univariate Cox regression analysis (with $P < 0.05$).

Establishment of predictive model and survival analysis

The 504 patients were randomly divided into a training set and a validation set. There were no significant differences in clinical characteristics between the training and validation cohorts (Table 1). Then, 19 prognostic FRLs

Table 1 Clinical information of 504 patients with LUAD from the TCGA database

Clinical features	TCGA database (n = 504)	Training group (n = 252)	Validation group (n = 252)
Age	65.30 ± 10.03	65.26 ± 9.91	65.34 ± 10.17
Sex			
Male	234	122	112
Female	270	130	140
Pathological stage			
I	270	137	133
II	119	62	57
III	81	38	43
IV	26	12	14
Unknown	8	3	5
T			
T1	168	77	91
T2	269	137	132
T3	45	25	20
T4	19	11	8
Unknown	3	2	1
N			
N0	325	162	163
N1	94	50	44
N2	71	30	41
N3	2	1	1
Unknown	12	9	3
M			
M0	335	163	172
M1	25	12	13
Unknown	144	77	67

selected by the LASSO algorithm were used to calculate the RS, and the formula is shown below (Fig. 3a-b). $RS = \exp[(-0.155689001) *LINC01908 + (-0.048007678) *LINC00582 + (-0.966427117) *MED4-AS1 + (-0.060758065) *AC034102.8 + (0.043720579) *AL049836.1 + (0.104812457) *AC087588.1 + (-0.155348446) *AC090559.1 + (-0.110255866) *AC026355.2 + (-0.035440534) *AL161618.1 + (-0.064732213) *FAM30A + (-0.01945136) *MHENCR + (-0.240780809) *AC006017.1 + (0.390969837) *AC010175.1 + (0.210496796) *KTN1-AS1 + (0.613005188) *AC009226.1 + (0.073272911) *AL606489.1 + (0.031857583) *AC009275.1 + (0.040530768) *AC069542.1 + (0.079655558) *AC084117.1]. After the LASSO algorithm, the area under the ROC curve (AUC) of the model for 1-year, 3-year, and 5-year OS was 0.763, 0.745, and 0.778 in the training set and 0.716, 0.724, and 0.736 in the validation set, respectively (Fig. 3c-d). The ROCs of clinical features are also shown in Fig. 3e-f. After Cox regression analysis, RS and stage were both considered significant predictive factors for the OS of patients with LUAD in all groups (Table 2). Then, a nomogram based on RS and stage was established, and an ROC curve was drawn (Fig. 3g, Additional file 1). According to the median value of the RS, the survival status was shown based on the two risk groups, and the OS of the high-risk group was significantly poorer than that of the low-risk group in both the training set ($P < 0.001$) and test set ($P < 0.001$), as shown in Fig. 4a-h. The optimized subset of prognostic FRLs in the coexpression network and the relationship with FRGs were visualized using the circle map and Sankey diagram (Fig. 5a-b). The differential analysis of each clinical feature in the two risk groups is shown in the heatmap, and the stage of patients with LUAD was significantly different (Fig. 5c).$

GSEA

GSEA revealed that the set of genes was enriched in the cell cycle, pyrimidine metabolism and RNA degradation for the high-risk group (Fig. 6a-c). In the low-risk group, the gene set was mainly enriched for asthma, intestinal immune network for IgA production and hematopoietic cell lineage (Fig. 6d-f).

(See figure on next page.)

Fig. 3 Building the prognostic model and nomogram. **a, b** The process of LASSO regression which added a penalty term for shrinkage of the parameter estimates to the least-squares loss function; **c-f** the ROC of prognostic model and clinical features for 5-years OS in the training set (**c, e**) and validation set (**d, f**); **g** the nomogram based on clinical features and prognostic model for OS of patients with LUAD. The red highlights showed that the total point of the patient with LUAD who was Stage IV was 48.8 and the probability of survival time of the patient less than 1, 3, 5 years was 0.212, 0.635, 0.894, respectively

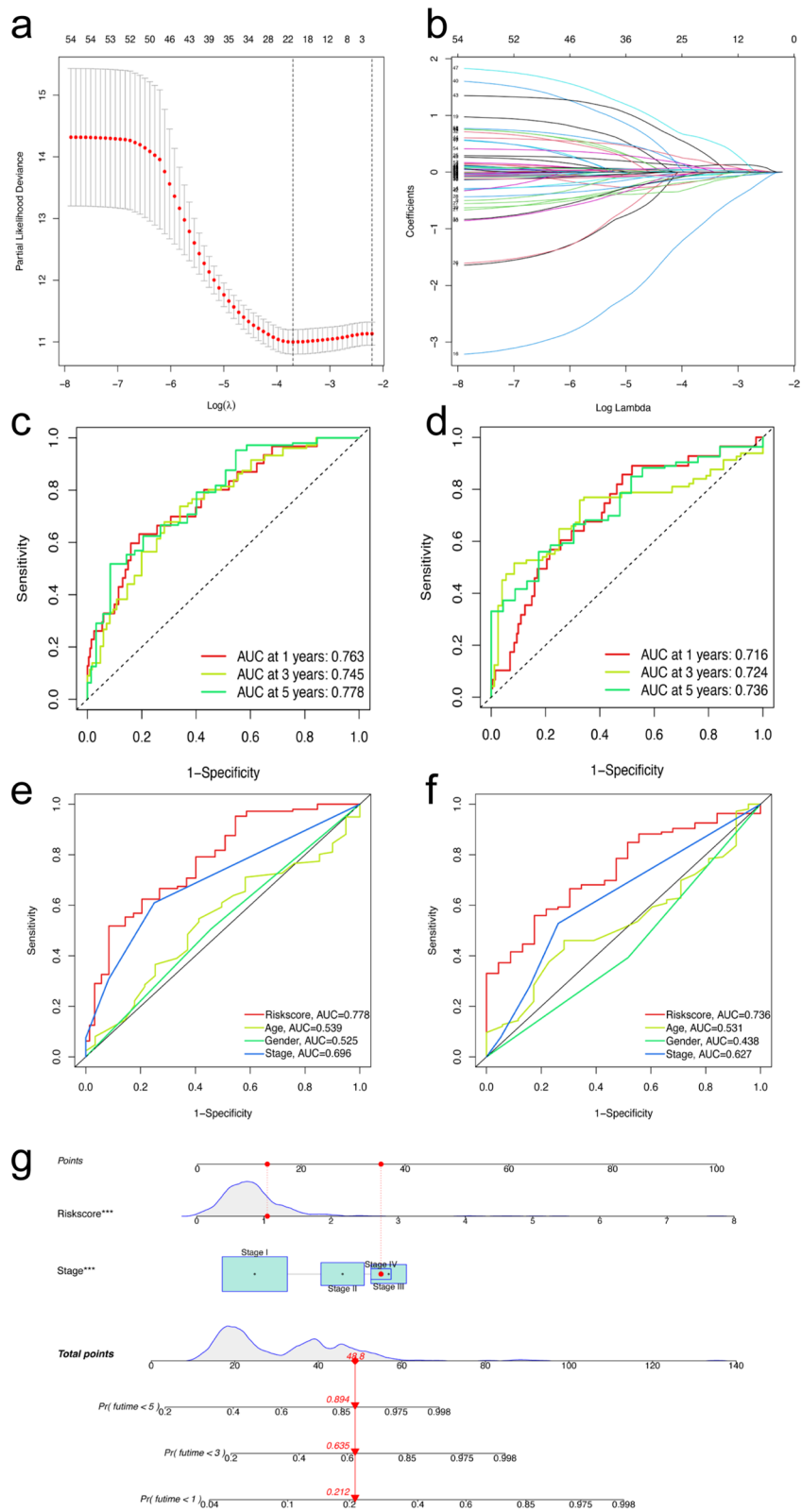


Fig. 3 (See legend on previous page.)

Table 2 Univariate and multivariate Cox regression analysis

Variable	Univariate Cox regression		Multivariate Cox regression	
	HR (95% CI)	P value	HR (95% CI)	P value
Training cohort				
Age	1.013 (0.990–1.036)	0.261	1.032 (1.007–1.057)	0.011
Sex	1.444 (0.935–2.228)	0.097	1.317 (0.849–2.043)	0.218
Stage	1.763 (1.431–2.171)	<0.001	1.803 (1.435–2.266)	<0.001
Risk score	2.405 (1.952–2.964)	<0.001	2.444 (1.964–3.040)	<0.001
Test cohort				
Age	1.004 (0.983–1.024)	0.734	1.005 (0.985–1.025)	0.631
Sex	0.867 (0.575–1.308)	0.497	0.837 (0.544–1.287)	0.417
Stage	1.526 (1.265–1.842)	<0.001	1.557 (1.285–1.887)	<0.001
Risk score	1.718 (1.435–2.056)	<0.001	1.734 (1.438–2.093)	<0.001

CI: confidence interval; HR, Hazard ratio

Differential immune analysis of RS

A heatmap of immune infiltration based on the TIMER, CIBERSORT, CIBERSORT-ABS, QUANTISEQ, MCP-COUNTER, XCELL and EPIC tools is shown in Fig. 7a. The results of the comparative analysis of immune function between the two risk groups are shown by the box-plot (Fig. 7b). The expression of 34 checkpoint genes was significantly different between the two risk groups (Fig. 7c).

Differential expression analysis of m6A

The difference in the expression level of m6A-related genes between the two risk groups is shown in Fig. 7d. The expressions of 13 m6A-related genes were significantly different between two risk groups. The expression levels of VIRMA, HNRNPC, HNRNPA2B1, IGF2BP1, IGF2BP2, IGF2BP3 and LRPPRC were significantly higher in the high-risk group ($P < 0.001$). The expression level of YTHDC2 was significantly lower in the high-risk group ($P < 0.001$).

Discussion

After univariate Cox regression analysis and the LASSO algorithm, 19 prognostic FRLs were established in the model for predicting the OS of patients with LUAD. Those with LUAD were separated by the median value of the RS. The high-risk group showed significantly worse OS than the low-risk group ($P < 0.001$). Univariate and

multivariate Cox regression revealed that a valuable significant risk factor was RS. The results of the differential immune analysis indicated that the RS was correlated with immune cell infiltration in our study. In addition, the differential expression of m6A-related genes in the two-risk group could indicate that FRLs were associated with these m6A-related genes in the prognosis of patients with LUAD. This study is the first to comprehensively analyze FRLs in the prognosis of patients with LUAD, immune cell infiltration and m6A modification.

Many studies have shown that lncRNAs can regulate ferroptosis in the oncogenesis and progression of malignant tumors [29–31]. A study by Zhang et al. showed that OIP5-AS1 could promote cell growth and inhibit ferroptosis in prostate cancer, which functioned as a competing source of endogenous RNAs (ceRNAs) for miR-128-3p to regulate the expression of SLC7A11 [29]. A study by Mao et al. showed that P53RRA could lead to ferroptosis by retaining p53 in the nucleus and serves as a tumor suppressor by displacing p53 from a cytosolic G3BP1 complex [30]. A study by Wu et al. showed that NEAT1 could modulate the expression of ACSL4 in NSCLC, which was a FRL in previous reports, and further affect the ferroptosis process [31]. These studies indicated that FRLs could contribute to the tumorigenesis and progression of malignant tumors, regulate ferroptosis and influence the invasion of tumors. However, few studies have examined how FRLs affect the progression of LUAD. In this study, the gene set of FRLs from patients with LUAD was mainly enriched in the cell cycle, pyrimidine metabolism and RNA degradation in the high-risk group, which had significantly worse OS than the low-risk group. These results indicated that FRLs could affect the progression of patients with LUAD and the OS of patients with LUAD.

In our study, 19 prognostic FRLs were confirmed to build the prediction model of patients with LUAD. A total of 8 out of 19 FRLs, which included LINC00582, MED4-AS1, AC090559.1, AL161618.1, FAM30A, MHENCR, KTN1-AS1 and AL606489.1, were previously investigated in tumors [32–39]. The results of both Wu et al. and Guo et al. showed that the expression of AC090559.1 was higher and the expression of AL606489.1 was lower in the low-risk group, and these two lncRNAs were both considered significant predictive factors for the OS of patients with LUAD [32, 33]. These findings are in line with the results of our study. The study of Li et al. showed that KTN1-AS1 expression was upregulated in NSCLC tissue and was positively correlated with poor prognosis, which could be considered a ceRNA for miR-130a-5p to regulate NSCLC cell growth and apoptosis [34]. These findings are also in line with the results of our study. In addition, Lima et al. showed that the expression of FAM30A was positively associated with

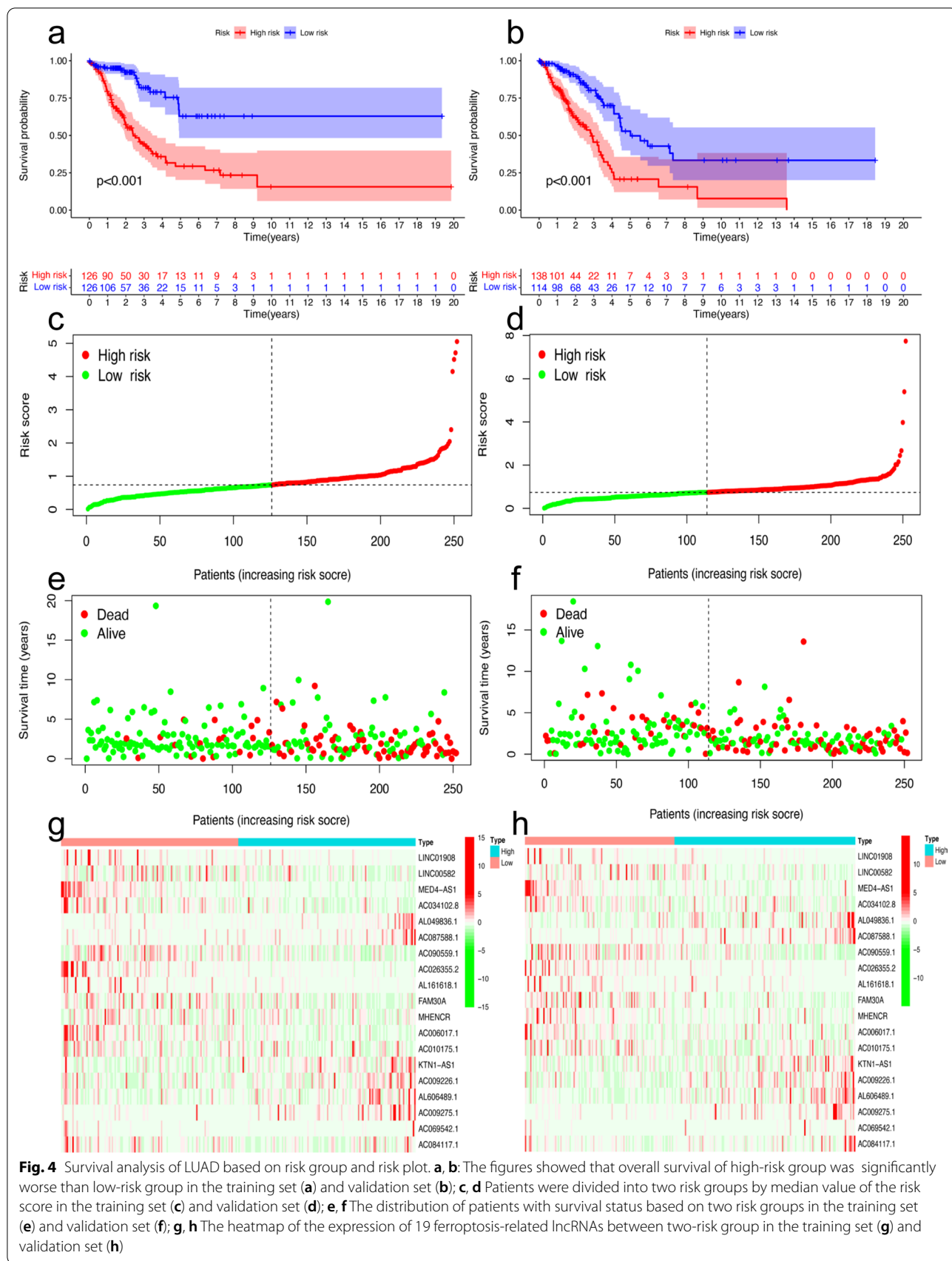


Fig. 4 Survival analysis of LUAD based on risk group and risk plot. **a, b** The figures showed that overall survival of high-risk group was significantly worse than low-risk group in the training set (**a**) and validation set (**b**); **c, d** Patients were divided into two risk groups by median value of the risk score in the training set (**c**) and validation set (**d**); **e, f** The distribution of patients with survival status based on two risk groups in the training set (**e**) and validation set (**f**); **g, h** The heatmap of the expression of 19 ferroptosis-related lncRNAs between two-risk group in the training set (**g**) and validation set (**h**)

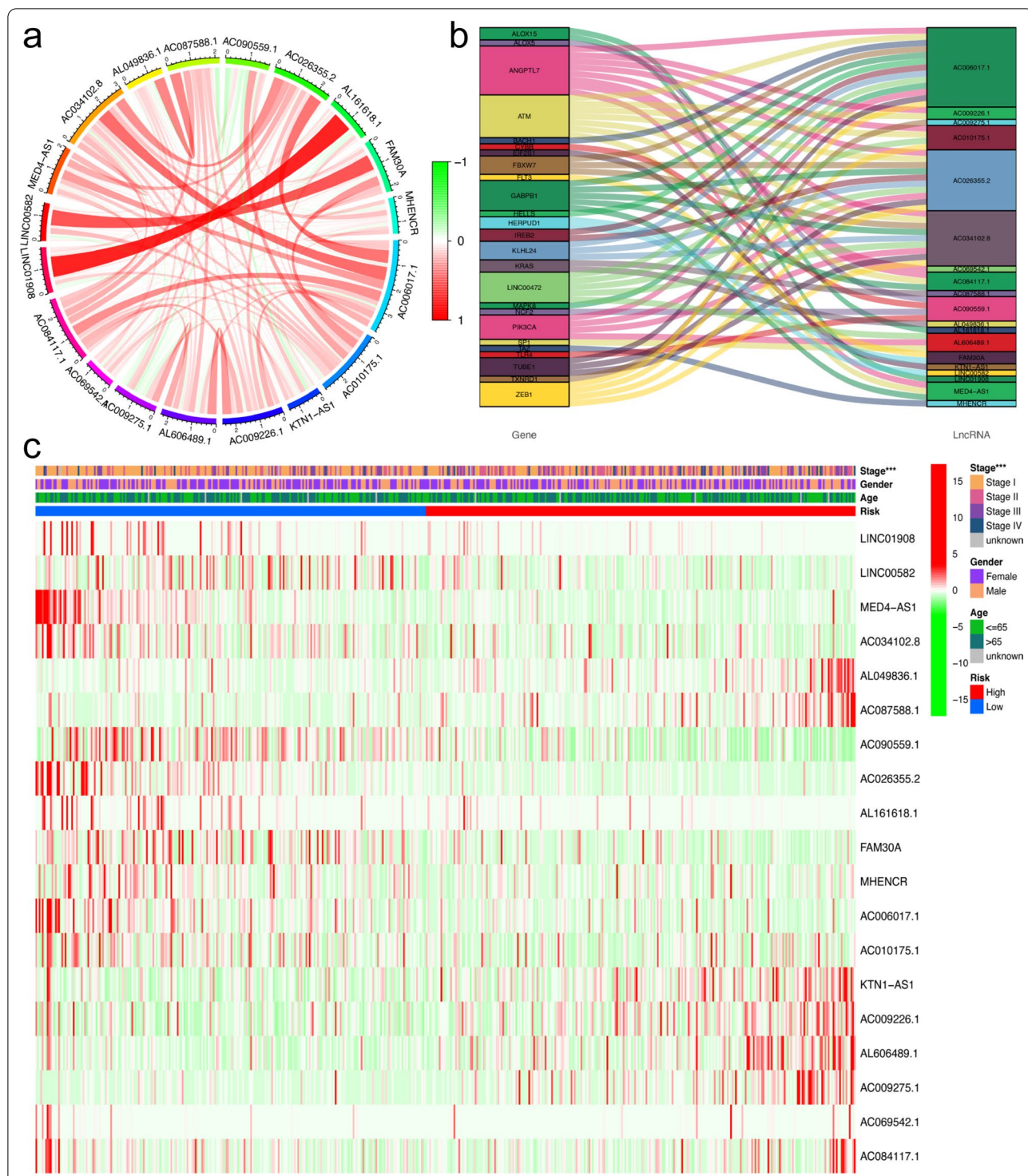
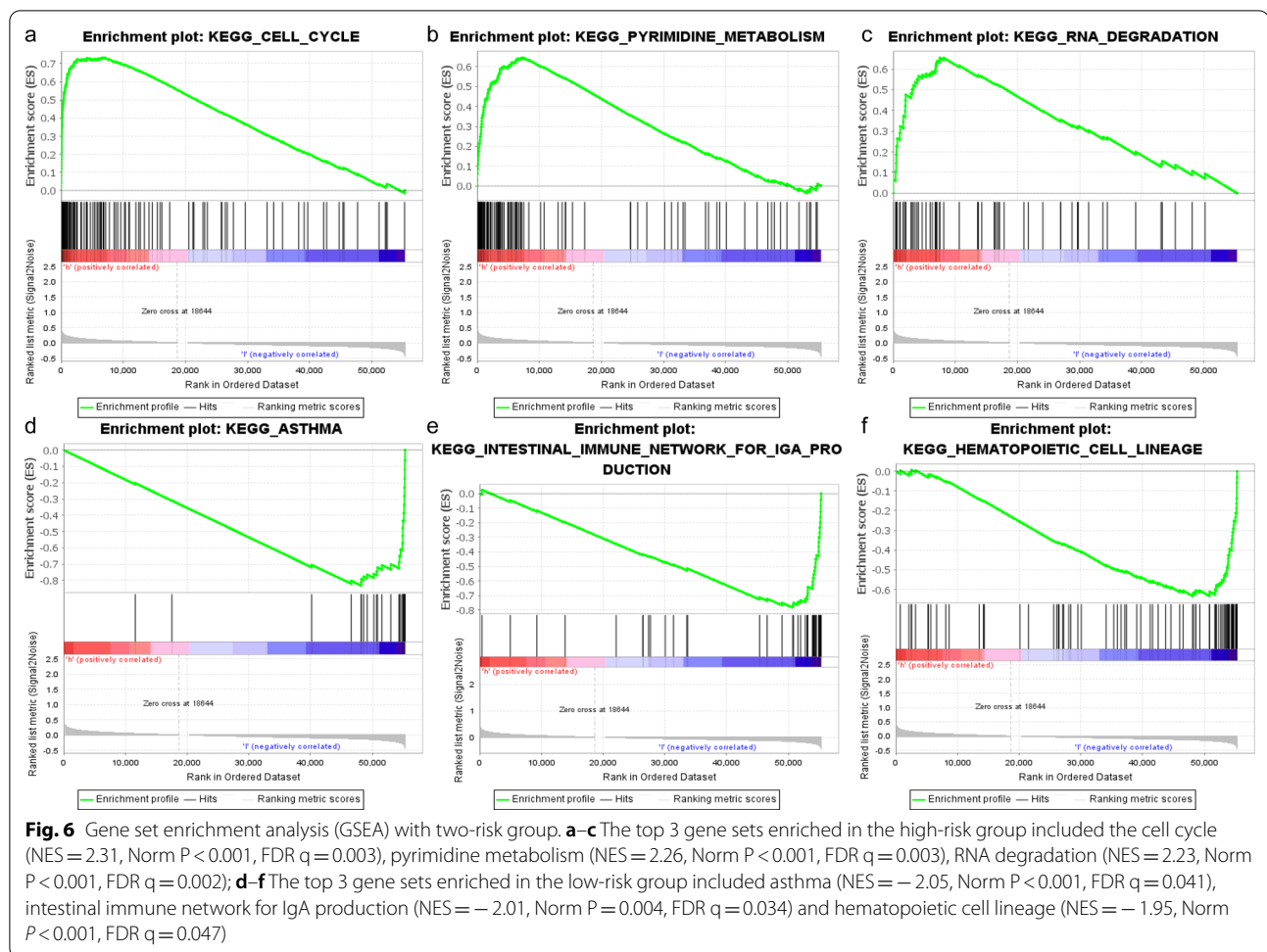


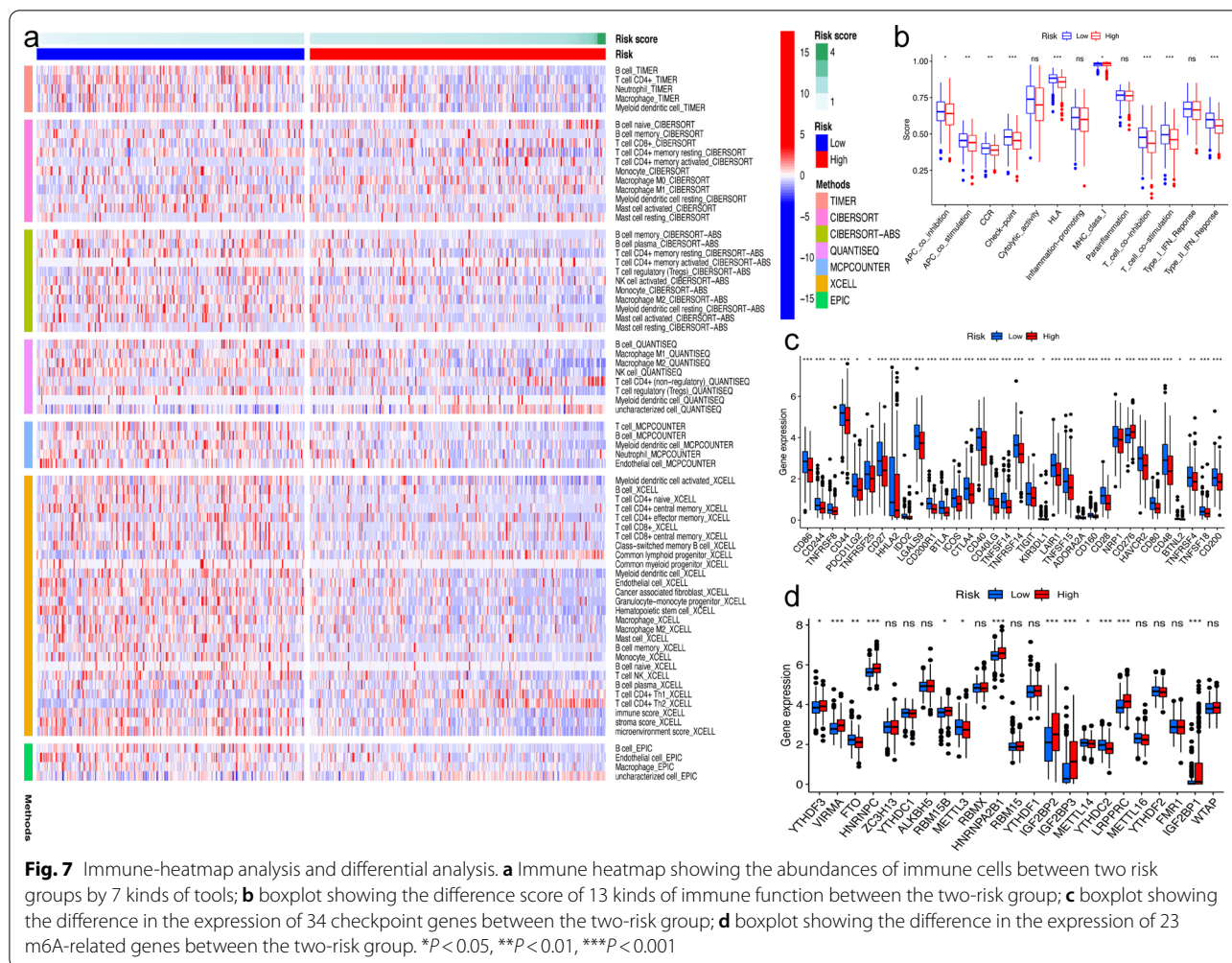
Fig. 5 Correlation analysis based on risk group in all patients. **a** Circle map showing the optimized subset of prognostic ferroptosis-related lncRNAs (FRLs) in the coexpression network. The bar represented the correlation. The thickness of the line indicates the strength of the correlation coefficient. **b** Sankey diagram showing the coexpression of ferroptosis-related genes and 19 FRLs. **c**: The figure shows that the patients in the two-risk group were significantly different in these subgroups of patients with stage of disease. The heatmap also showed the 19 FRL expressions in the two-risk group. * $P < 0.05$, ** $P < 0.01$, *** $P < 0.001$



the level of antibody titers and the lncRNA might regulate immunoglobulin heavy locus gene segments [35]. Furthermore, several studies have shown that abnormal immune cells contribute to the progression of LUAD and regulate ferroptosis, and checkpoint inhibitor-based immunotherapies have improved the survival of patients with advanced malignancies [40–44]. In our study, significant differences in immune cell infiltration and function and the expression of immune checkpoints between the two risk groups were also confirmed to a certain extent. A parallel study by Yao et al. identified 7 FRLs that had diagnostic utility in OS for patients with LUAD, and the results showed that the AUCs of the risk model based on 7 FRLs for 1 year, 2 years, and 3 years were 0.711, 0.658, and 0.676 in the training set and 0.593, 0.577, and 0.525 in the validation set [45]. A net of 7 FRL differences was determined in their study, while a net of 19 FRL differences was determined in our study. What's more, stage III had a slightly higher point than stage IV in the nomogram of our study. The reason may be the differences between several sample sets and the TCGA cohort and

insufficient sample size. However, overwhelming evidence suggests that the identified FRLs hold high diagnostic utility in the oncogenesis of LUAD, and further studies along this direction are needed.

On a separate note, several studies have investigated the relationship between m6A modification and the prognosis of LUAD [22, 46, 47]. A study by Ma et al. demonstrated that YTHDC2, a m6A-related gene, could suppress HOXA13 by m6A modification to suppress SLC3A2 and further promote ferroptosis in LUAD [22]. In addition, a study by Xu et al. demonstrated that the risk model, which was considered an independent indicator for the prognosis of LUAD, was composed of 12 m6A-related lncRNAs, and the AUC of the risk model was 0.759 [46]. It is evident that modification of m6A was able to influence the progression of cancers. Our study showed that the expression levels of 13 m6A-related genes between the two-risk group were significantly different. The results indicated that m6A modification could play a potential role in FRLs in the prediction of the prognosis of patients with LUAD, and further



research is needed to obtain more details about undying associations.

While significant findings were reported above, limitations to these findings are described below. First, the use of independent LUAD cohorts or multiple databases would increase the diagnostic power and improve the nomogram over a single TCGA dataset. Second, in vitro and in vivo experiments should be used in conjunction to determine the mechanistic function of FRLs in oncogenesis.

Conclusions

In summary, this study determined the prognostic value of FRLs in LUAD patients and used these findings to generate a prognostic model to effectively predict the OS of patients with LUAD. Moreover, a nomogram for a predictive prognostic model was built, and the differential expression of m6A-related genes in the two-risk group was confirmed. As such, the FRLs identified herein may suggest therapeutic targets for the treatment of LUAD.

Abbreviations

AUC: Area under the receiver operating characteristic curve; BP: Biological process; CC: Cellular component; CI: Confidence interval; DEGs: Differential expression genes; EPIC: Estimating the proportion of immune and cancer cells; FDR: False discovery rate; FRGs: Ferroptosis-related genes; FRLs: Ferroptosis-related long noncoding RNAs; GO: Gene ontology; GRCh38: Genome Reference Consortium Human Build 38; GSEA: Gene set enrichment analysis; HR: Hazard ratio; KEGG: Kyoto Encyclopedia of Genes and Genomes; KM: Kaplan–Meier; LASSO: Least absolute shrinkage and selection operator; lncRNAs: Long noncoding RNAs; LUAD: Lung adenocarcinoma; m6A: N6-methyladenosine; MCPOUNTER: Microenvironment cell populations-counter; MF: Molecular function; NES: Normalized enrichment score; Norm: Normalized; OS: Overall survival; ROC: Receiver operating characteristic; RS: Risk score; TCGA: The Cancer Genome Atlas.

Supplementary Information

The online version contains supplementary material available at <https://doi.org/10.1186/s12920-022-01164-5>.

Additional file 1. The ROC of nomogram.

Additional file 2. The data analysis.

Acknowledgements

We thank the contributions of the TCGA project.

Authors' contributions

All authors contributed to this paper. CG and NK: Investigation, Formal analysis, Data Curation, Software, Visualization, Writing—Original Draft. FZ: Investigation, Formal analysis, Visualization. TT: Data Curation, Software, Validation. JL: Formal analysis, Visualization. HD: Formal analysis, Visualization. ZS: Formal analysis, Visualization. LW and MX: Conceptualization, Methodology, Resources, Writing—Reviewing and Editing, Supervision, Project administration. All authors read and approved the final paper.

Funding

This work was supported by the Medical Health Science and Technology Project of Zhejiang Provincial Health Commission (2022KY230, 2019KY117, WKJ-ZJ-2039) and the Zhejiang Provincial Natural Science Foundation of China (LSY19H180003).

Availability of data and materials

All data, including the transcriptome profiling normalization data and the relevant clinical features, were acquired from the Genomic Data Commons Data Portal (<https://portal.gdc.cancer.gov>) of TCGA, which is the open access data. The data analysis was also included in the Additional file 2.

Declarations

Ethics approval and consent to participate

TCGA belongs to public databases. The patients involved in the database obtained ethical approval. Users can download relevant data for free for research and publish relevant articles. Our study is based on open access data, so there are no ethical issues or other conflicts of interest.

Consent for publication

Not applicable.

Competing interests

The authors declare that they have no competing interests.

Author details

¹Department of Radiology, The First Affiliated Hospital of Zhejiang Chinese Medical University (Zhejiang Provincial Hospital of Traditional Chinese Medicine), 54 Youdian Road, Hangzhou, China. ²The First School of Clinical Medicine, Zhejiang Chinese Medical University, Hangzhou, China. ³Zhejiang Provincial Key Laboratory of Pancreatic Disease, The First Affiliated Hospital, School of Medicine, Zhejiang University, Hangzhou, Zhejiang, China. ⁴Department of Hepatobiliary and Pancreatic Surgery, The First Affiliated Hospital, School of Medicine, Zhejiang University, Hangzhou, Zhejiang, China.

Received: 16 September 2021 Accepted: 24 January 2022

Published online: 29 January 2022

References

- Siegel RL, Miller KD, Fuchs HE, Jemal A. Cancer statistics, 2021. *CA Cancer J Clin.* 2021;71(1):7–33. <https://doi.org/10.3322/caac.21654>.
- Allemani C, Matsuda T, Di Carlo V, Harewood R, Matz M, Nikšić M, et al. Global surveillance of trends in cancer survival 2000–14 (CONCORD-3): analysis of individual records for 37 513 025 patients diagnosed with one of 18 cancers from 322 population-based registries in 71 countries. *Lancet.* 2018;391(10125):1023–75. [https://doi.org/10.1016/S0140-6736\(17\)33326-3](https://doi.org/10.1016/S0140-6736(17)33326-3).
- Herbst RS, Morgensztern D, Boshoff C. The biology and management of non-small cell lung cancer. *Nature.* 2018;553(7689):446–54. <https://doi.org/10.1038/nature25183>.
- Lee JJ, Park S, Park H, Kim S, Lee J, Lee J, et al. Tracing oncogene rearrangements in the mutational history of lung adenocarcinoma. *Cell.* 2019;177(7):1842–1857.e21. <https://doi.org/10.1016/j.cell.2019.05.013>.
- Hirsch FR, Scagliotti GV, Mulshine JL, Kwon R, Curran WJ Jr, Wu YL, et al. Lung cancer: current therapies and new targeted treatments. *Lancet.* 2017;389(10066):299–311. [https://doi.org/10.1016/S0140-6736\(16\)30958-8](https://doi.org/10.1016/S0140-6736(16)30958-8).
- Yu P, Tong L, Song Y, Qu H, Chen Y. Systematic profiling of invasion-related gene signature predicts prognostic features of lung adenocarcinoma. *J Cell Mol Med.* 2021;25(13):6388–402. <https://doi.org/10.1111/jcmm.16619>.
- Li J, Cao F, Yin HL, Huang ZJ, Lin ZT, Mao N, et al. Ferroptosis: past, present and future. *Cell Death Dis.* 2020;11(2):88. <https://doi.org/10.1038/s41419-020-2298-2>.
- Chen X, Kang R, Kroemer G, Tang D. Broadening horizons: the role of ferroptosis in cancer. *Nat Rev Clin Oncol.* 2021;18(5):280–96. <https://doi.org/10.1038/s41571-020-00462-0>.
- Wu Y, Zhang S, Gong X, Tam S, Xiao D, Liu S, et al. The epigenetic regulators and metabolic changes in ferroptosis-associated cancer progression. *Mol Cancer.* 2020;19(1):39. <https://doi.org/10.1186/s12943-020-01157-x>.
- Zhou N, Bao J. FerrDb: a manually curated resource for regulators and markers of ferroptosis and ferroptosis-disease associations. *Database (Oxford).* 2020. <https://doi.org/10.1093/database/baaa021>.
- Tang Z, Jiang W, Mao M, Zhao J, Chen J, Cheng N. Deubiquitinase USP35 modulates ferroptosis in lung cancer via targeting ferroportin. *Clin Transl Med.* 2021;11(4): e390. <https://doi.org/10.1002/ctm2.390>.
- Wohlhieter CA, Richards AL, Uddin F, Hulton CH, Quintanal-Villalonga A, Martin A, et al. Concurrent mutations in STK11 and KEAP1 promote ferroptosis protection and SCD1 dependence in lung cancer. *Cell Rep.* 2020;33(9): 108444. <https://doi.org/10.1016/j.celrep.2020.108444>.
- Zhu G, Huang H, Xu S, Shi R, Gao Z, Lei X, et al. Prognostic value of ferroptosis-related genes in patients with lung adenocarcinoma. *Thorac Cancer.* 2021;12(12):1890–9. <https://doi.org/10.1111/1759-7714.13998>.
- Statello L, Guo CJ, Chen LL, Huarte M. Gene regulation by long non-coding RNAs and its biological functions. *Nat Rev Mol Cell Biol.* 2021;22(2):96–118. <https://doi.org/10.1038/s41580-020-00315-9>.
- Wang Z, Chen X, Liu N, Shi Y, Liu Y, Ouyang L, et al. A Nuclear long non-coding RNA LINC00618 accelerates ferroptosis in a manner dependent upon apoptosis. *Mol Ther.* 2021;29(1):263–74. <https://doi.org/10.1016/j.ymthe.2020.09.024>.
- Wang M, Mao C, Ouyang L, Liu Y, Lai W, Liu N, et al. Long noncoding RNA LINC00336 inhibits ferroptosis in lung cancer by functioning as a competing endogenous RNA. *Cell Death Differ.* 2019;26(11):2329–43. <https://doi.org/10.1038/s41418-019-0304-y>.
- Zaccara S, Ries RJ, Jaffrey SR. Reading, writing and erasing mRNA methylation. *Nat Rev Mol Cell Biol.* 2019;20(10):608–24. <https://doi.org/10.1038/s41580-019-0168-5>.
- Xiong X, Hou L, Park YP, Molin B, GTEX Consortium, Gregory RI, et al. Genetic drivers of m6A methylation in human brain, lung, heart and muscle. *Nat Genet.* 2021; <https://doi.org/10.1038/s41588-021-00890-3>
- Li F, Wang H, Huang H, Zhang L, Wang D, Wan Y. m6A RNA methylation regulators participate in the malignant progression and have clinical prognostic value in lung adenocarcinoma. *Front Genet.* 2020;11:994. <https://doi.org/10.3389/fgene.2020.00994>.
- Ma L, Chen T, Zhang X, Miao Y, Tian X, Yu K, et al. The m6A reader YTHDC2 inhibits lung adenocarcinoma tumorigenesis by suppressing SLC7A11-dependent antioxidant function. *Redox Biol.* 2021;38: 101801. <https://doi.org/10.1016/j.redox.2020.101801>.
- Hao CC, Xu CY, Zhao XY, Luo JN, Wang G, Zhao LH, et al. Up-regulation of VANG1 by IGF2BPs and miR-29b-3p attenuates the detrimental effect of irradiation on lung adenocarcinoma. *J Exp Clin Cancer Res.* 2020;39(1):256. <https://doi.org/10.1186/s13046-020-01772-y>.
- Ma L, Zhang X, Yu K, Xu X, Chen T, Shi Y, et al. Targeting SLC3A2 subunit of system XC- is essential for m6A reader YTHDC2 to be an endogenous ferroptosis inducer in lung adenocarcinoma. *Free Radic Biol Med.* 2021;168:25–43. <https://doi.org/10.1016/j.freeradbiomed.2021.03.023>.
- Li T, Fu J, Zeng Z, Cohen D, Li J, Chen Q, et al. TIMER2.0 for analysis of tumor-infiltrating immune cells. *Nucleic Acids Res.* 2020;48(W1):W509–W514. <https://doi.org/10.1093/nar/gkaa407>
- Newman AM, Liu CL, Green MR, Gentles AJ, Feng W, Xu Y, et al. Robust enumeration of cell subsets from tissue expression profiles. *Nat Methods.* 2015;12(5):453–7. <https://doi.org/10.1038/nmeth.3337>.
- Finotello F, Mayer C, Plattner C, Laschober G, Rieder D, Hackl H, et al. Molecular and pharmacological modulators of the tumor immune contexture revealed by deconvolution of RNA-seq data. *Genome Med.* 2019;11(1):34. <https://doi.org/10.1186/s13073-019-0638-6>.

26. Becht E, Giraldo NA, Lacroix L, Buttard B, Elarouci N, Petitprez F, et al. Estimating the population abundance of tissue-infiltrating immune and stromal cell populations using gene expression. *Genome Biol.* 2016;17(1):218. <https://doi.org/10.1186/s13059-016-1070-5>.
27. Aran D, Hu Z, Butte AJ. xCell: digitally portraying the tissue cellular heterogeneity landscape. *Genome Biol.* 2017;18(1):220. <https://doi.org/10.1186/s13059-017-1349-1>.
28. Racle J, Gfeller D. EPIC: a tool to estimate the proportions of different cell types from bulk gene expression data. *Methods Mol Biol.* 2020;2120:233–48. https://doi.org/10.1007/978-1-0716-0327-7_17 (PMID: 32124324).
29. Zhang Y, Guo S, Wang S, Li X, Hou D, Li H, et al. LncRNA OIP5-AS1 inhibits ferroptosis in prostate cancer with long-term cadmium exposure through miR-128-3p/SLC7A11 signaling. *Ecotoxicol Environ Saf.* 2021;220: 112376. <https://doi.org/10.1016/j.ecoenv.2021.112376>.
30. Mao C, Wang X, Liu Y, Wang M, Yan B, Jiang Y, et al. A G3BP1-interacting lncRNA promotes ferroptosis and apoptosis in cancer via nuclear sequestration of p53. *Cancer Res.* 2018;78(13):3484–96. <https://doi.org/10.1158/0008-5472.CAN-17-3454>.
31. Wu H, Liu A. Long non-coding RNA NEAT1 regulates ferroptosis sensitivity in non-small-cell lung cancer. *J Int Med Res.* 2021;49(3):300060521996183. <https://doi.org/10.1177/0300060521996183>.
32. Wu L, Wen Z, Song Y, Wang L. A novel autophagy-related lncRNA survival model for lung adenocarcinoma. *J Cell Mol Med.* 2021;25(12):5681–90. <https://doi.org/10.1111/jcmm.16582>.
33. Guo Y, Qu Z, Li D, Bai F, Xing J, Ding Q, et al. Identification of a prognostic ferroptosis-related lncRNA signature in the tumor microenvironment of lung adenocarcinoma. *Cell Death Discov.* 2021;7(1):190. <https://doi.org/10.1038/s41420-021-00576-z>.
34. Li C, Zhao W, Pan X, Li X, Yan F, Liu S, et al. LncRNA KTN1-AS1 promotes the progression of non-small cell lung cancer via sponging of miR-130a-5p and activation of PDPK1. *Oncogene.* 2020;39(39):6157–71. <https://doi.org/10.1038/s41388-020-01427-4>.
35. de Lima DS, Cardozo LE, Maracaja-Coutinho V, Suhrbier A, Mane K, Jefries D, et al. Long noncoding RNAs are involved in multiple immunological pathways in response to vaccination. *Proc Natl Acad Sci U S A.* 2019;116(34):17121–6. <https://doi.org/10.1073/pnas.1822046116>.
36. Wang Z, Zhang J, Liu Y, Zhao R, Zhou X, Wang H. An integrated autophagy-related long noncoding rna signature as a prognostic biomarker for human endometrial cancer: a bioinformatics-based approach. *Biomed Res Int.* 2020;2020:5717498. <https://doi.org/10.1155/2020/5717498>.
37. Chen X, Dong H, Liu S, Yu L, Yan D, Yao X, et al. Long noncoding RNA MHENCR promotes melanoma progression via regulating miR-425/489-mediated PI3K-Akt pathway. *Am J Transl Res.* 2017;9(1):90–102.
38. Chen M, Zheng Y, Xie J, Zhen E, Zhou X. Integrative profiling analysis identifies the oncogenic long noncoding RNA DUXAP8 in oral cancer. *Anticancer Drugs.* 2020;31(8):792–8. <https://doi.org/10.1097/CAD.0000000000000936>.
39. Wang XW, Guo QQ, Wei Y, Ren KM, Zheng FS, Tang J, et al. Construction of a competing endogenous RNA network using differentially expressed lncRNAs, miRNAs and mRNAs in non-small cell lung cancer. *Oncol Rep.* 2019;42(6):2402–15. <https://doi.org/10.3892/or.2019.7378>.
40. Biton J, Mansuet-Lupo A, Pécuchet N, Alifano M, Ouakrim H, Arrondeau J, et al. TP53, STK11, and EGFR mutations predict tumor immune profile and the response to Anti-PD-1 in lung adenocarcinoma. *Clin Cancer Res.* 2018;24(22):5710–23. <https://doi.org/10.1158/1078-0432.CCR-18-0163>.
41. Kang L, Miao MS, Song YG, Fang XY, Zhang J, Zhang YN, et al. Total flavonoids of *Taraxacum mongolicum* inhibit non-small cell lung cancer by regulating immune function. *J Ethnopharmacol.* 2021;114514. doi:<https://doi.org/10.1016/j.jep.2021.114514>
42. Galland L, Le Page AL, Lecuelle J, Bibeau F, Oulkhovir Y, Derangère V, et al. Prognostic value of Thyroid Transcription Factor-1 expression in lung adenocarcinoma in patients treated with anti PD-1/PD-L1. *Oncimmunology.* 2021;10(1):1957603. <https://doi.org/10.1080/2162402X.2021.1957603>.
43. Wang W, Green M, Choi JE, et al. CD8+ T cells regulate tumour ferroptosis during cancer immunotherapy. *Nature.* 2019;569(7755):270–4. <https://doi.org/10.1038/s41586-019-1170-y>.
44. Lang X, Green MD, Wang W, et al. Radiotherapy and immunotherapy promote tumoral lipid oxidation and ferroptosis via synergistic repression of SLC7A11. *Cancer Discov.* 2019;9(12):1673–85. <https://doi.org/10.1158/2159-8290.CD-19-0338>.
45. Yao J, Chen X, Liu X, Li R, Zhou X, Qu Y. Characterization of a ferroptosis and iron-metabolism related lncRNA signature in lung adenocarcinoma. *Cancer Cell Int.* 2021;21(1):340. <https://doi.org/10.1186/s12935-021-02027-2>.
46. Xu F, Huang X, Li Y, Chen Y, Lin L. m6A-related lncRNAs are potential biomarkers for predicting prognoses and immune responses in patients with LUAD. *Mol Ther Nucleic Acids.* 2021;24:780–91. <https://doi.org/10.1016/j.omtn.2021.04.003>.
47. Wang H, Zhao X, Lu Z. m6A RNA Methylation Regulators Act as Potential Prognostic Biomarkers in Lung Adenocarcinoma. *Front Genet.* 2021;12: 622233. <https://doi.org/10.3389/fgene.2021.622233>.

Publisher's Note

Springer Nature remains neutral with regard to jurisdictional claims in published maps and institutional affiliations.

Ready to submit your research? Choose BMC and benefit from:

- fast, convenient online submission
- thorough peer review by experienced researchers in your field
- rapid publication on acceptance
- support for research data, including large and complex data types
- gold Open Access which fosters wider collaboration and increased citations
- maximum visibility for your research: over 100M website views per year

At BMC, research is always in progress.

Learn more biomedcentral.com/submissions

